

Article

Coherent Chaotic Communication Using Generalized Runge–Kutta Method

Ivan Babkin ¹, Vyacheslav Rybin ², Valery Andreev ¹, Timur Karimov ¹ and Denis Butusov ^{2,*}

¹ Computer-Aided Design Department, St. Petersburg Electrotechnical University “LETI”, 5 Professora Popova St., 197022 Saint Petersburg, Russia; iababkin@etu.ru (I.B.); vsandreev@etu.ru (V.A.); tikarimov@etu.ru (T.K.)

² Youth Research Institute, St. Petersburg Electrotechnical University “LETI”, 5 Professora Popova St., 197022 Saint Petersburg, Russia; vgrybin@etu.ru

* Correspondence: dnbutusov@etu.ru

Abstract: Computer simulation of continuous chaotic systems is usually performed using numerical methods. The discretization may introduce new properties into finite-difference models compared to their continuous prototypes and can therefore lead to new types of dynamical behavior exhibited by discrete chaotic systems. It is known that one can control the dynamics of a discrete system using a special class of integration methods. One of the applications of such a phenomenon is chaos-based communication systems, which have recently attracted attention due to their high covertness and broadband transmission capability. Proper modulation of chaotic carrier signals is one of the key problems in chaos-based communication system design. It is challenging to modulate and demodulate a chaotic signal in the same way as a conventional signal due to its noise-like shape and broadband characteristics. Therefore, the development of new modulation–demodulation techniques is of great interest in the field. One possible approach here is to use adaptive numerical integration, which allows control of the properties of the finite-difference chaotic model. In this study, we describe a novel modulation technique for chaos-based communication systems based on generalized explicit second-order Runge–Kutta methods. We use a specially designed test bench to evaluate the efficiency of the proposed modulation method and compare it with state-of-the-art solutions. Experimental results show that the proposed modulation technique outperforms the conventional parametric modulation method in both coverage and noise immunity. The obtained results can be efficiently applied to the design of advanced chaos-based communication systems as well as being used to improve existing architectures.

Keywords: chaos; chaotic signal modulation; coherent communication system; Runge–Kutta method

MSC: 68N30; 65P20; 65Y10; 39A33



Citation: Babkin, I.; Rybin, V.; Andreev, V.; Karimov, T.; Butusov, D. Coherent Chaotic Communication Using Generalized Runge–Kutta Method. *Mathematics* **2024**, *12*, 994. <https://doi.org/10.3390/math12070994>

Academic Editor: Lingfeng Liu

Received: 8 March 2024

Revised: 24 March 2024

Accepted: 25 March 2024

Published: 27 March 2024



Copyright: © 2024 by the authors. Licensee MDPI, Basel, Switzerland. This article is an open access article distributed under the terms and conditions of the Creative Commons Attribution (CC BY) license (<https://creativecommons.org/licenses/by/4.0/>).

1. Introduction

Chaos-based communication is a promising technology for secure and efficient transmission of information and utilizes the unique properties of chaotic dynamics. One of the recently emerging topics in the field of communication engineering is the design and implementation of digital chaotic communication systems [1]. Such systems are supposed to use discrete chaos generators to achieve secure and efficient transmission of information via various physical channels. Chaotic dynamics are characterized by their nonlinearity, complexity, unpredictability, and sensitivity to initial conditions and parameters, which results in specific behavior that appears to be similar to random noise but is deterministic and reproducible by nature. Chaotic signals can be generated by relatively simple discrete models that are obtained by discretizing some well-known chaotic systems such as the Lorenz system [2,3] or the logistic equation [4]. Analog chaos can be found in such physical devices as lasers [5–7], electronic circuits [8,9], or neurons [10].

The main idea behind chaotic communication systems is to use chaotic signals, also referred to as chaotic carriers, to encode and decode the transmitted information [11]. Chaotic signals possess several desirable properties for covert communication purposes, such as broad bandwidth, robustness to noise and interference, and low correlation with other signals. Moreover, chaotic signals can provide a natural way of encrypting the information to protect from possible tampering or eavesdropping, as they are difficult to distinguish from noise, predict, or reconstruct without knowing the exact parameters and initial conditions of the underlying chaotic system [12]. Therefore, chaotic communication systems can offer a high level of security and privacy for the transmitted data.

However, chaotic communication systems (CCSs) also face several important limitations that need to be addressed and overcome for successful design. One of the main challenges in constructing so-called coherent CCSs is the issue of synchronization between the transmitter and the receiver, which is essential for coherent detection and decoding of the information [13]. Synchronization is the process of achieving identical or clearly correlated dynamics between two or more chaotic systems and can be achieved by various methods such as direct coupling by the Pecora–Carroll technique [14], feedback control [15], or parameter adaptation [16]. It should be noted that, despite the use of chaotic carriers allowing the creation of robust, secure, and covert communication systems, several pitfalls prevent the widespread adoption of chaotic systems for this type of communication. First, the generation, transmission, and denoising of chaotic signals are complicated tasks that require special mathematics and should be approached with care [17]. Second, the sensitive nature of chaotic dynamics increases the impact of discretization on the properties of the finite difference model. The interesting fact is that the discrete model of a continuous chaotic system may not only lack some of the known properties of the original system but may also exhibit new behavior that was not present in the original system [18]. Another challenging problem is the lack of efficient techniques for modulating chaotic signals. Modulation is the process of varying one or more properties of a chaotic system, which generates the carrier signal, by following a separate sequence called the modulation signal that typically contains information to be transmitted and can be done in various ways, such as chaos shift keying [19], chaotic masking [20], parameter modulation [21,22], symmetry coefficient modulation [22], and others. For non-coherent CCSs, one can mention differential chaos shift keying [23], quadrature chaos shift keying [24], and differential chaos shift keying code division multiple access [25]. Besides obvious robustness and easy implementation, non-coherent chaotic communication systems are not always able to provide high-level covertness for the transmitted information. Therefore, this study pays attention mainly to coherent communication systems.

The choice of modulation scheme affects the performance and security level of the chaotic communication system as well as the complexity and cost of implementation. Modulation of chaotic signals requires high robustness to be able to change modulation parameters without breaking the desired oscillation mode and high resistivity to noise in the communication channel. Several secure communication schemes based on chaotic dynamics have been reported in the recent literature. Pisarchik et al. introduced a secure communication system based on extreme multistability [26]. Joseph Chang Lun Chan et al. presented a chaotic secure communication scheme using a sliding-mode observer [27]. YuYan Bian et al. [28] constructed a new six-dimensional Lorenz hyperchaotic system. The authors analyzed the equilibrium stability, dissipation, bifurcation, and Lyapunov exponent spectrum of the hyperchaotic system to verify its chaotic behavior. The simulation results indicate that the proposed scheme takes 0.45 s to synchronize, and the encryption method exhibits high security of transmission. Ouannas et al. propose a new secure communications approach that is obtained by combining into one scheme the chaotic modulation, recursive encryption, and chaotic masking [20]. Oscar Martínez-Fuentes et al. [29] implemented a secure communication system for image encryption using the Raspberry Pi platform with MQTT for IoT protocol for transmission.

Some other studies have been conducted on the use of chaotic oscillators in Internet of Things applications. Cirjulina et al. [30] analyzed the characteristics and operational aspects of chaos oscillators with a focus on low-power functionality, resilient chaotic oscillations, and resistance to parameter variations and noise. This analysis was aimed at advancing secure communication methodologies for wireless sensor networks in the Internet of Things and highlights the significance of chaotic dynamics for ensuring robust and secure data transmission. Benkhaddra Ilyas et al. presented a hyperchaos-based reconfigurable platform for real-time security of communicating embedded systems interconnected in networks following the Internet of Things (IoT) standards [31].

It should be noted that there are relatively few studies dedicated to hardware implementations of chaotic communication systems. Saudi et al. [32] developed a new optimal and simple approach for real-time implementation of continuous chaotic generator systems on a field programmable gate array (FPGA). The authors used the fourth-order Runge–Kutta method to obtain a discrete chaotic generator based on a well-known Chen system. Sahin et al. presented a memristor-based hyperchaotic circuit and implemented it in communication systems based on the same FPGA platform [33]. The signals obtained from the memristor-based hyperchaotic system have been utilized for both analog and digital communication schemes in this hardware solution and are a good demonstration of the nonlinearity of the memristor. Elsafty et al. performed a comprehensive study on the effect of using different floating-point representations on the chaotic system's behavior [34]. Pano-Azucena [35] showed that a numerical method based on trigonometric polynomials provides better accuracy than forward Euler and, as also shown herein, requires lower FPGA resources compared to fourth-order RK. The proposed FPGA hardware realization for the new Wang chaotic system includes integer, floating-point, and fixed-point components. This implementation achieves a significant reduction in hardware resources: approximately 10 times less than in previous works.

Speaking of coherent chaotic systems, the synchronization of chaotic signals becomes a keystone procedure. Since Pecora and Carroll [36] demonstrated that it was possible to synchronize chaotic circuits, there has been a significant amount of research dedicated to studying the phenomenon of synchronization. Babajans et al. examined the potential for synchronization between analog and discrete models of the Vilnius chaotic oscillator [37] and evaluated the efficiency of the Pecora–Carroll synchronization method for achieving synchronization between analog and discrete chaos oscillators [38]. Karimov et al. demonstrated the practical possibility of synchronization between digital and analog chaotic circuits, achieving synchronization accuracy higher than in the analog-to-analog case [39]. Weidong Shao et al. created a chaotic synchronization scheme based on electro–optical hybrid entropy sources [40].

In our previous papers, we presented a new modulation principle that utilizes the variable properties of a discrete integration operator for signal modulation. Karimov et al. [22] introduced symmetry coefficient modulation (SCM), which uses the unique properties of symmetric numerical integration methods with adaptive symmetry. In [41,42], Tutueva et al. described an approach to adaptive synchronization by controlling the symmetry coefficient. Rybin et al. [43] proposed effective numerical estimation of CCS secrecy based on a modified return map analysis. Previous works have shown high potential for CCSs that use signal modulation methods based on the controllable properties of the discrete operator. However, using symmetric integration in embedded solutions is not always suitable due to the possible implicitness of the resulting finite-difference models, which, in turn, causes extra computational costs. Therefore, in this paper, we present a simple and reliable CCS based on a generalized explicit second-order Runge–Kutta solver.

The main contributions of this study can be summarized as follows:

1. We investigate the nonlinear properties of a finite-difference model of the Gokyildirim et al. system obtained using a generalized explicit second-order Runge–Kutta solver. The discovered phenomenon of artificial multistability is explored using the Lyapunov spectrum, bifurcation analysis, and basin of attraction analysis.

2. We present a novel modulation technique called alpha modulation (αM), which is suitable for constructing coherent chaos-based communication systems. The proposed technique assumes the controllable value of α in the generalized explicit second-order Runge–Kutta solver and corresponding discrete chaotic map obtained from a continuous system. The prototype system is based on the Gokyildirim et al. chaotic system. The experiments were performed using the Arduino-based CCS test bench developed by the authors.
3. The experimental results indicate that data transfer using αM is feasible. The system’s performance was evaluated by comparing several important properties and included noise resistivity and secrecy superior to those of parameter modulation (PM) implemented on the same hardware.
4. The study employed the quantified return map analysis (QRMA) technique to evaluate the secrecy of the communication system. We discovered that while the noise resistivity among all the investigated modulation techniques is similar, the symmetry modulation technique exhibits greater secrecy than parametric modulation and variable midpoint modulation.

The rest of the paper is organized as follows. In Section 2, a description of two generalized Runge–Kutta methods is given, and the test chaotic system is introduced. Bifurcation and LLE analysis are performed to analyze the multistable behavior of a chosen system. Section 3 describes and investigates the architecture of the designed chaotic communication system with a new modulation type in comparison with known solutions. Finally, Section 4 concludes the paper.

2. Materials and Methods

2.1. Second-Order Runge–Kutta Methods

There are many known methods belonging to the Runge–Kutta family that possess second-order algebraic accuracy [44]. A famous example of a second-order method with two stages is the explicit midpoint method:

$$y_{n+1} = y_n + hf(t_n + \frac{h}{2}, y_n + \frac{h}{2}f(t_n, y_n)). \tag{1}$$

Another well-known example is the explicit trapezoidal rule, also known as Heun’s method [45]:

$$y_{n+1} = y_n + \frac{h}{2}f(t_n, y_n) + \frac{h}{2}f(t_n + h, y_n + hf(t_n, y_n)). \tag{2}$$

Also, Ralston’s method [46] is broadly used:

$$y_{n+1} = y_n + \frac{h}{4}f(t_n, y_n) + \frac{3h}{4}f(t_n + \frac{2h}{3}, y_n + \frac{2h}{3}f(t_n, y_n)). \tag{3}$$

All these methods are explicit second-order Runge–Kutta ODE solvers. Let us write the generalized formula for the second-order explicit Runge–Kutta method with newly introduced parameter α :

$$y_{n+1} = y_n + h((1 - \frac{1}{2\alpha})f(t_n, y_n) + \frac{1}{2\alpha}f(t_n + \alpha h, y_n + \alpha hf(t_n, y_n))). \tag{4}$$

The Butcher table for the generalized second-order explicit Runge–Kutta method is as follows:

$$\begin{array}{c|c} 0 & \alpha \\ \alpha & \alpha \\ \hline & | (1 - \frac{1}{2\alpha}) \quad \frac{1}{2\alpha} \end{array}$$

In two-stage form, the method holds:

$$\begin{aligned} k_1 &= f(t_n, y_n); \\ k_2 &= f(t_n + \alpha h, y_n + \alpha h f(y_n)); \\ y_{n+1} &= y_n + h(\alpha_1 k_1 + \alpha_2 k_2); \end{aligned} \tag{5}$$

where $\alpha_1 = 1 - \frac{1}{2\alpha}$, $\alpha_2 = \frac{1}{2\alpha}$.

In one of our previous studies [47], we investigated the case of controlling the midpoint position in the midpoint method. Note that while it is reasonable to select a range of midpoint positions for the variable $m \in [0, 1]$, choosing midpoint values outside this range may result in additional changes in the dynamics and lead to interesting new behavior not typical for the prototype system. However, it is important to note that selecting a midpoint value other than 0.5 could lead to a decrease in the stability and convergence of the finite-difference model, which reduces the practical applicability of a controllable midpoint position for chaotic signal modulation tasks. Nevertheless, the proposed RK-alpha method is free from the above-mentioned shortcomings. According to its decomposition into Taylor series,

$$k_2 = f(t_n, y_n) + \alpha h f'(t_n, y_n) + O((\alpha h)^2) \tag{6}$$

One can substitute (6) into (5) to obtain:

$$\begin{aligned} y_{n+1} &= y_n + h\left(\left(1 - \frac{1}{2\alpha}\right)f(t_n, y_n) + \frac{h}{2\alpha}f'(t_n, y_n) + \frac{h^2}{2}f''(t_n, y_n) + O((\alpha h)^2)\right) = \\ &= y_n + hf(t_n, y_n) + \frac{h^2}{2}f'(t_n, y_n) + O((\alpha h)^2). \end{aligned} \tag{7}$$

As one can see from (7), a variable α does not present in the final series expansion and influences only the truncation error. Thus, it is generally valid to select the value of α arbitrarily. Usually, it is supposed that $\alpha \in (0, 1]$, which corresponds well with the geometrical interpretation of the method. Nevertheless, it is not necessary to choose α from this range to preserve the second order of accuracy. The dynamics exhibited by a discrete system at α values beyond the range of $(0, 1]$ are of particular interest. Interactions with the adaptive discrete operator can generate some nonlinear phenomena in the discrete model behavior that are not present in its continuous prototype. For example, in [18], the authors described the possibility of inducing artificial multistability in a discrete Chen system using composition diagonally implicit integration methods with controllable symmetry. Therefore, the hypothesis of the current study is that changing the parameter α can lead to similar changes in system dynamics.

2.2. Analysis of the Gokyildirim Discrete Model

In this study, we used the Gokyildirim et al. chaotic oscillator [48] as a mathematical model for designing the discrete chaos generator. This system is newly reported and has not been thoroughly explored yet; therefore it is of great interest for both theoretical studies and possible applications. The Gokyildirim oscillator is described by the following system of ordinary differential equations:

$$\begin{aligned} \dot{x} &= y + xy - yz; \\ \dot{y} &= x + ayz; \\ \dot{z} &= by^2 + xy; \end{aligned} \tag{8}$$

where $a = 0.1$, $b = 0.7$.

The finite-difference model of the system was obtained by applying the RK-alpha integration method (5) to system (8):

$$\begin{aligned}
 h_\alpha &= \alpha h; \\
 x_{n+\alpha} &= x_n + h_\alpha(y_n + x_n y_n - y_n z_n); \\
 y_{n+\alpha} &= y_n + h_\alpha(x_n + a y_n z_n); \\
 z_{n+\alpha} &= z_n + h_\alpha(b y_n^2 + x_n y_n); \\
 x_{n+1} &= x_n + h(\alpha_1(y_n + x_n y_n - y_n z_n) + \alpha_2(y_{n+\alpha} + x_{n+\alpha} y_{n+\alpha} - y_{n+\alpha} z_{n+\alpha})); \\
 y_{n+1} &= y_n + h(\alpha_1(x_n + a y_n z_n) + \alpha_2(x_{n+\alpha} + a y_{n+\alpha} z_{n+\alpha})); \\
 z_{n+1} &= z_n + h(\alpha_1(b y_n^2 + x_n y_n) + \alpha_2(b y_{n+\alpha}^2 + x_{n+\alpha} y_{n+\alpha})).
 \end{aligned}
 \tag{9}$$

where α is a value of the parameter alpha.

Let us investigate the influence of system (8)'s parameters on its dynamics. Figure 1 shows the two-dimensional bifurcation diagram (parametric chaotic set) plotted for parameters a and b . Note that the density-based spatial clustering of applications with noise (DBSCAN) clustering method for periodicity calculation was used to plot all the two-dimensional bifurcation diagrams in this study. The number of clusters is indicated by the color. The color on the two-dimensional bifurcation diagram indicates the complexity of the system dynamics: the closer the color is to red, the more chaotic behavior the system exhibits. It is reasonable to choose system parameters as close to red zones as possible for practical chaotic signal generation.

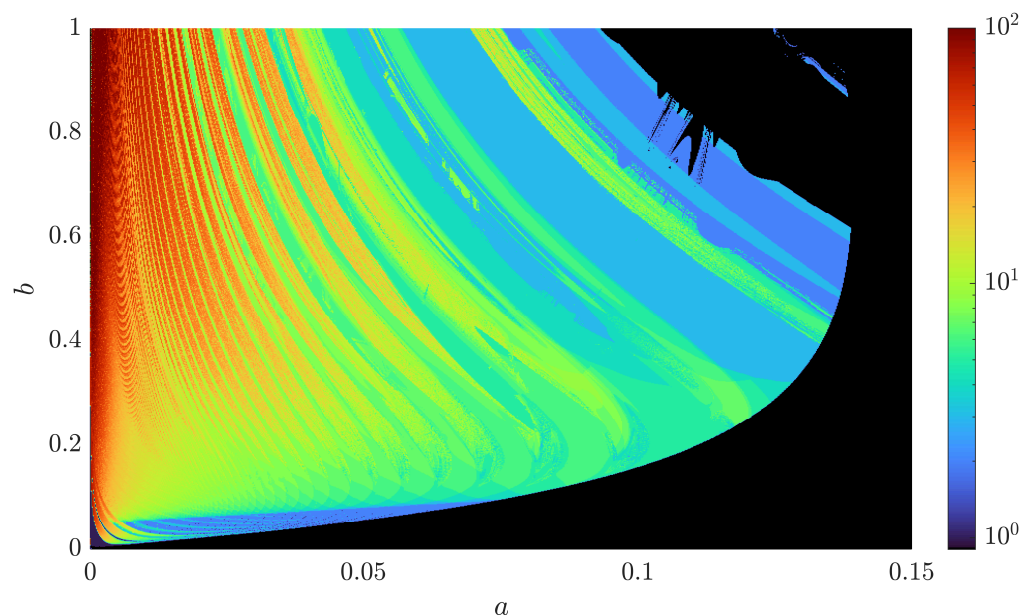


Figure 1. A 2D bifurcation diagram based on parameters a and b .

One can observe that multistable behavior exists in the investigated system for certain parameter combinations. Figure 2 shows the basins of attraction and the phase space for two sets of parameter values of the discrete Gokyildirim et al. system obtained using the RK-alpha integration method.

The next subsection investigates the dependence between the dynamics of the discrete system and the alpha parameter.

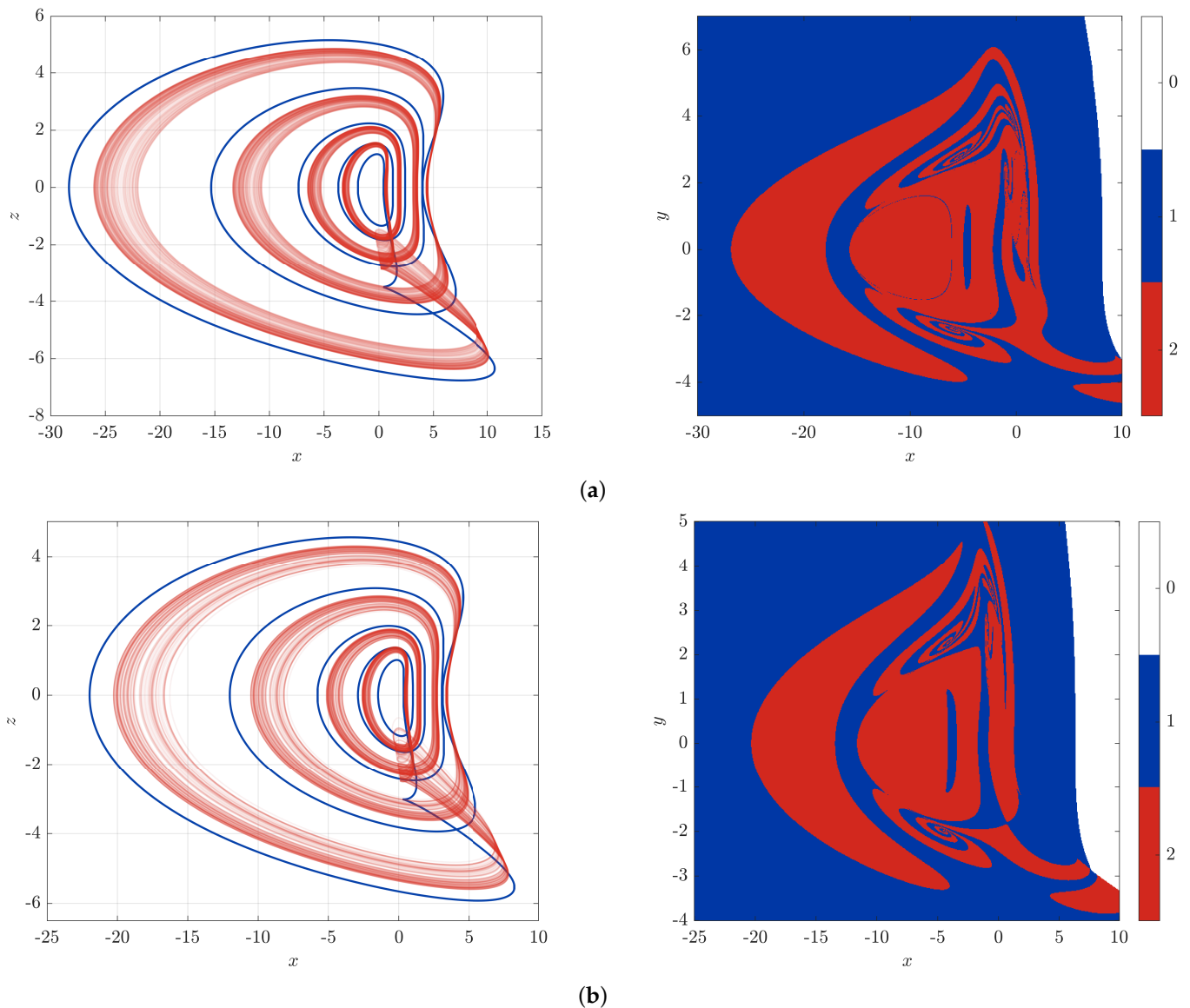


Figure 2. Basin of attraction and phase portrait for system (9). Red and blue colors correspond to two attractors, while the white color corresponds to the unbound solution; (a) $a = 0.065$ and $b = 0.45$, $z_0 = 0$; (b) $a = 0.0707$ and $b = 0.3955$, $z_0 = 0$.

2.2.1. The αh Bifurcation Diagram Analysis

Let us plot the bifurcation diagram of the considered system using the alpha parameter (see the bottom plot in Figure 3). One can see that the system exhibits stable chaotic and periodic oscillations even beyond the ranges of $\alpha \in (0, 1]$. The 2D bifurcation diagram shows how the dynamics of the system (8) depend on the integration step h and the value of α . However, a simple plot of $\alpha \times h$ will not clearly show all changes in the dynamics since the value α is multiplied by the integration step and thus will violate the scale because the range of the α values increases with the decrease in the integration step. Considering this, we used a technique similar to the method proposed in [18] for plotting two-dimensional $\alpha \times h$ diagrams as follows: for each integration step value, the range of the midpoint value is calculated according to the formula:

$$\alpha h^2 = const. \tag{10}$$

One can see that the stability of the obtained discrete map is preserved even outside the range of $\alpha \in (0, 1]$, allowing us to choose it arbitrarily. Figure 3 shows a 2D bifurcation

diagram that illustrates the dynamics of the system at various integration steps h while varying the value of α . The 1D bifurcation diagrams for $h = 0.002$, $h = 0.01$, and $h = 0.05$ are given as well.

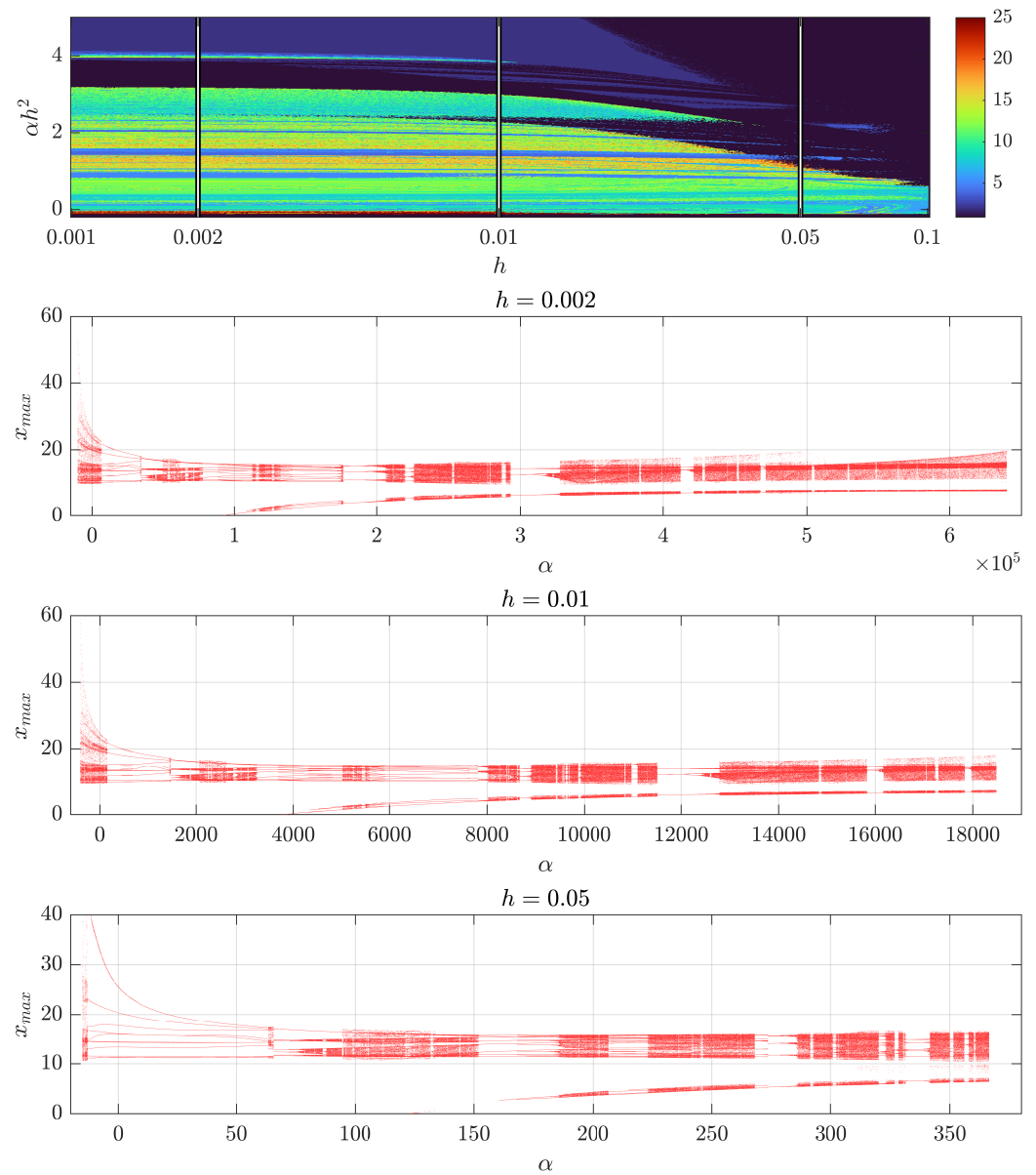


Figure 3. A 2D bifurcation diagram showing the dynamics of the system at various integration steps h while varying the value of α . Corresponding 1D bifurcation diagrams for α are given for different values of integration step h .

As one can see from Figure 3, varying the alpha parameter affects the dynamics of the oscillator. In the context of chaotic communication systems, it is important to choose alpha values that preserve the chaotic behavior of the oscillator on the transceiver side. The following subsections describe the bifurcation and Lyapunov spectrum analysis for investigation of the ranges of the α values that preserve the chaotic behavior of the system (8).

2.2.2. Bifurcation and Lyapunov Spectrum Analysis

For further experiments, the integration step h was chosen to be 0.01 s. Figure 4 shows the bifurcation diagram and Lyapunov spectrum illustrating the various dynamics

of the discrete Gokyildirim et al. system for different α values taken from a range between $\alpha = -400$ and $\alpha = 1000$.

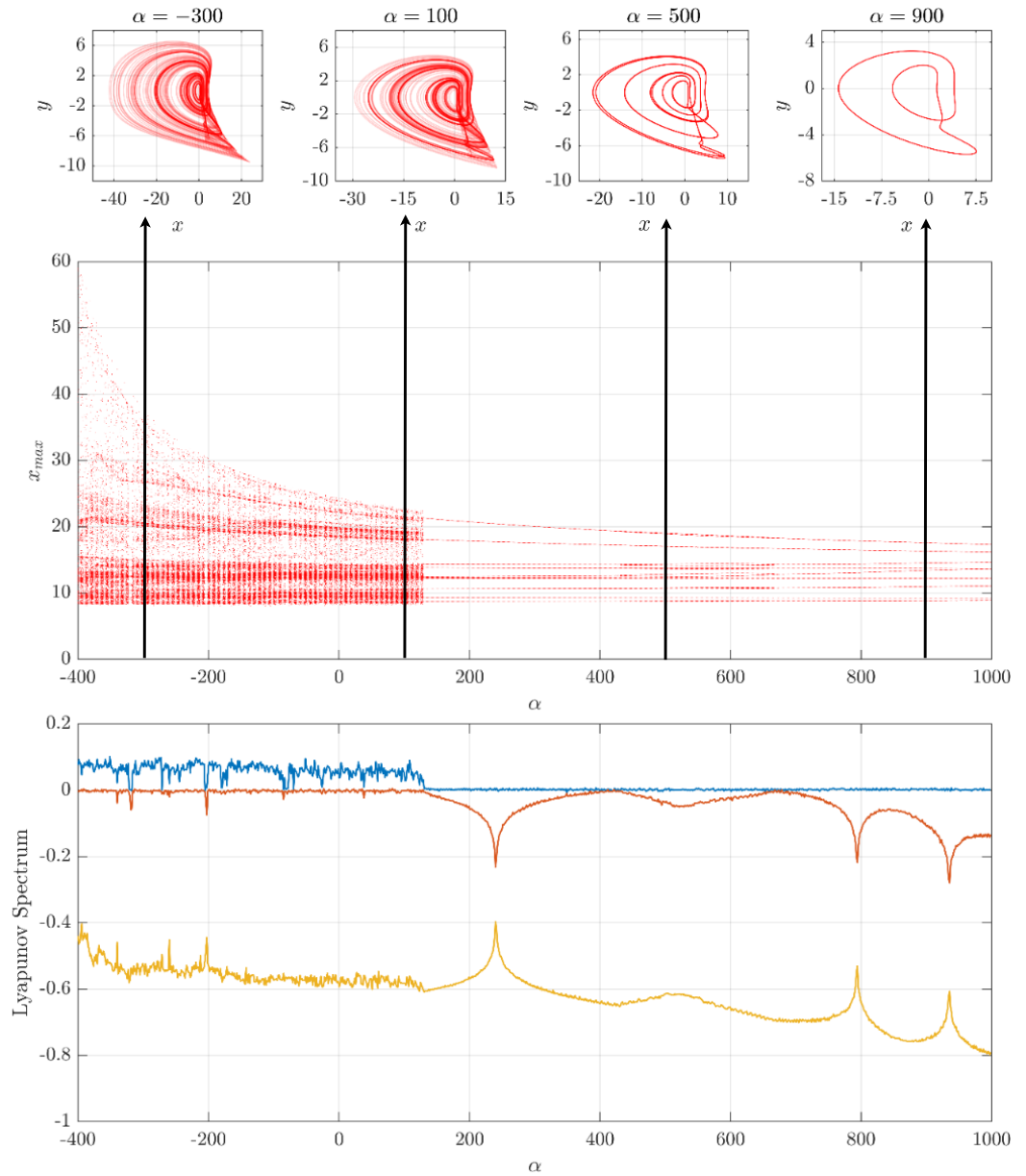


Figure 4. Bifurcation diagram and Lyapunov spectrum with respect to α . The phase portraits for different values of α are shown above.

Figure 5 shows a 2D bifurcation diagram with varying parameters a and α . The bifurcation diagram indicates the presence of both chaotic and periodic behavior. Additionally, Figure 6 presents phase portraits for various values of α and a .

Figure 7 shows a 2D bifurcation diagram for α and parameter b .

Figure 8 displays 2D bifurcation diagrams for different values of b for α and parameter a . It is evident that as the parameter b increases, the range of α values decreases.

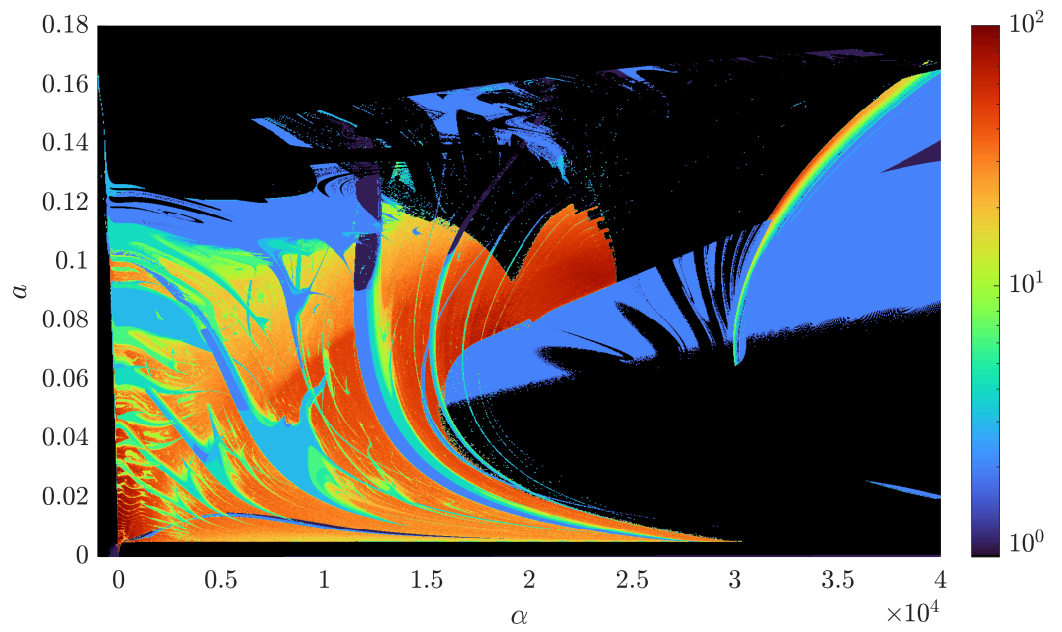


Figure 5. A 2D bifurcation diagram of α and parameter a .

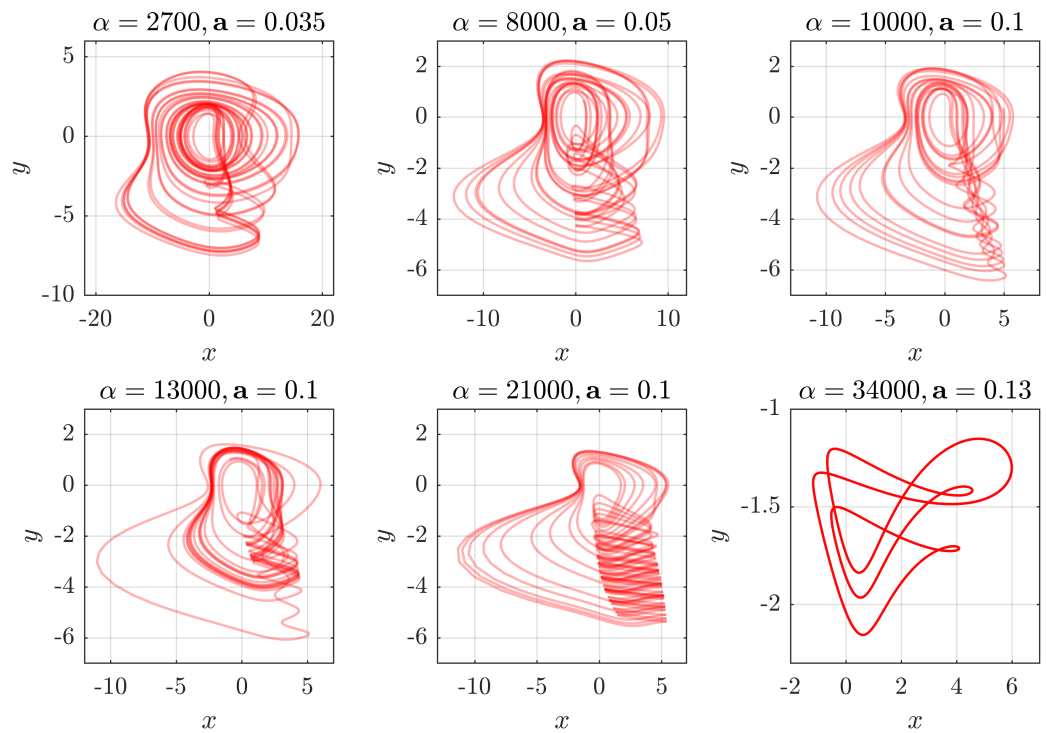


Figure 6. Phase portraits for different values of α and a .

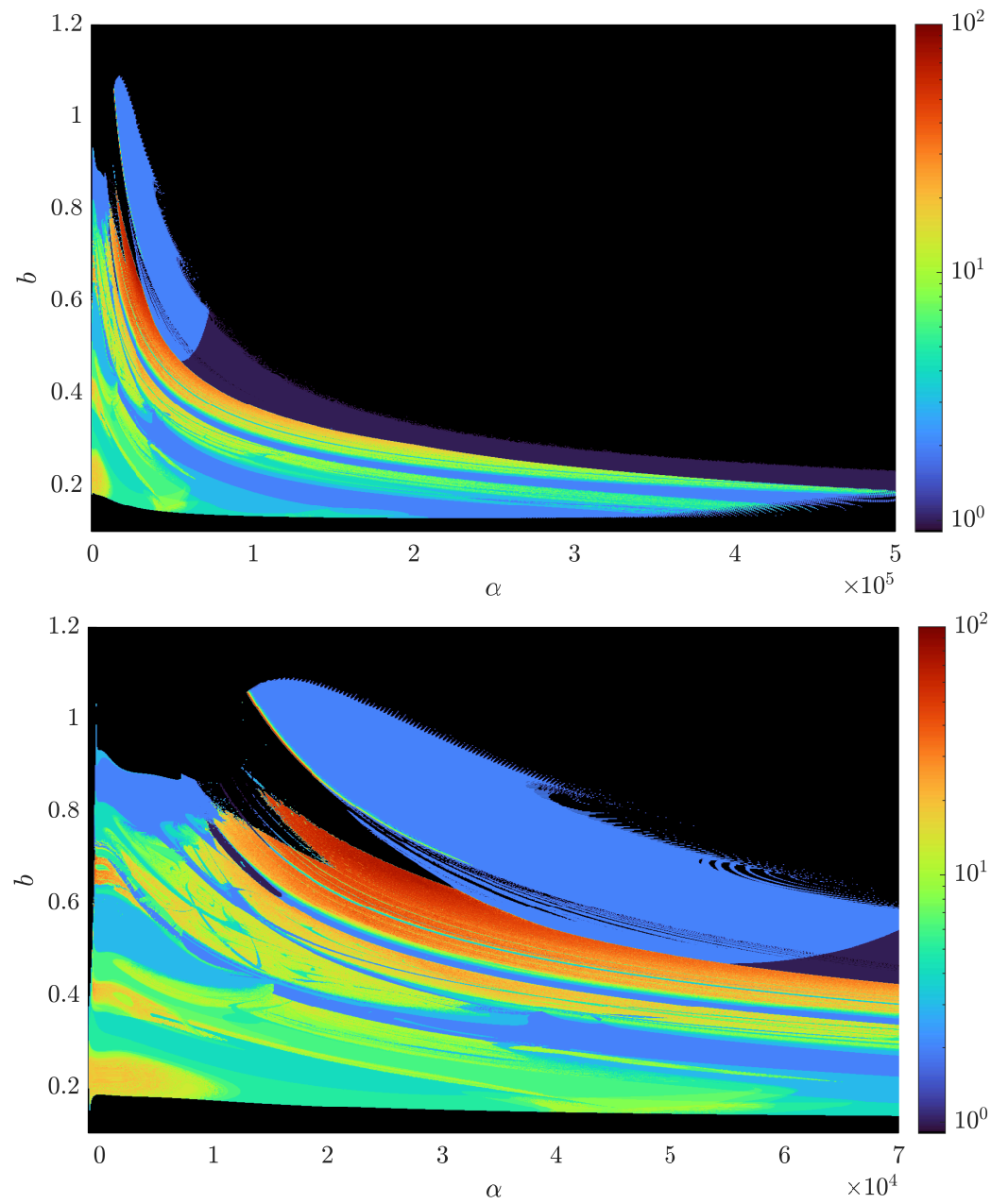


Figure 7. The 2D bifurcation diagrams for parameters α and b .

The features discovered in the dynamics of the discrete Gokyildirim et al. system during its analysis indicate that a coherent chaotic communication system can be constructed on its basis. Let us describe it by introducing a novel chaotic signal modulation technique.

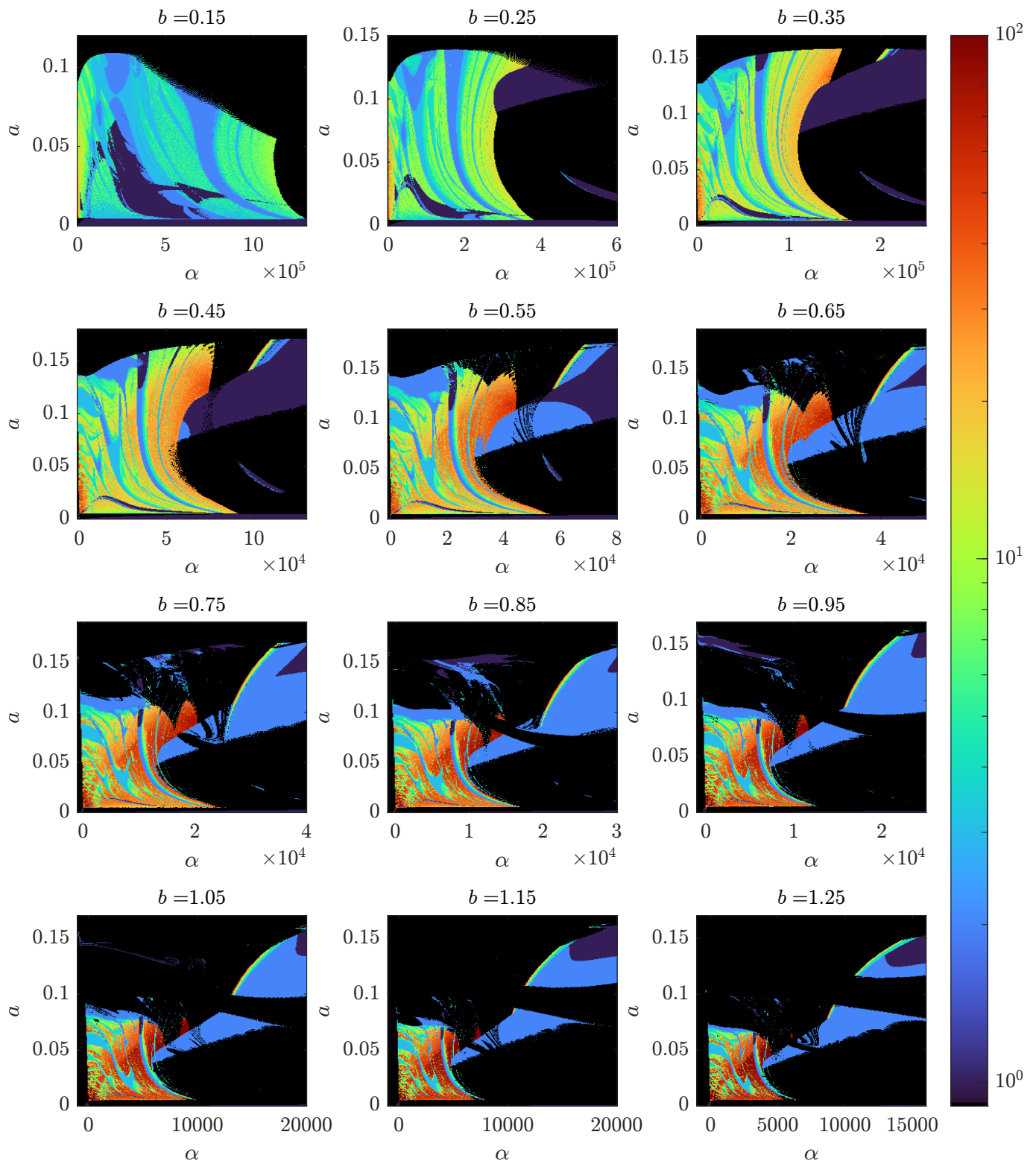


Figure 8. The 2D bifurcation diagrams for different values of b for α and parameter a .

3. Investigation of Chaotic Communication System with α -Based Signal Modulation

Let us consider a chaotic communication system based on the discrete Gokyildirim et al. system, obtained by the generalized explicit second-order Runge–Kutta solver, and with a new signal modulation method. The concept of using the numerical integration operator as a tool for modulating the chaotic signal generated by the corresponding discrete map is a recent development in CCS theory. In this section, we describe the principles of the

construction of a CCS based on the RK-alpha method. We present finite difference schemes for the receiver and the transmitter, and we describe a method for the evaluation of the covertness of the CCS under study. The principle of the chaos-based communication system can be described as follows. At the beginning, the digital information signal $m(t)$ modulates the RK-alpha value of the chaotic oscillator at the transmitter side. The signal then passes through the communication channel. White Gaussian noise is added in combination with the noise from the DAC and ADC units. We used 12-bit resolution ADC/DAC in our experiments. On the receiver side, depending on the transmitted message bit, the occurrence of generalized chaotic synchronization can be observed. The recovery of the message $M^*(t)$ is done by using the root mean square (RMS). In our previous work [49], we found that using RMS leads to the lowest BER values. A block diagram of the variable center point signal modulation communication system is shown in Figure 9.

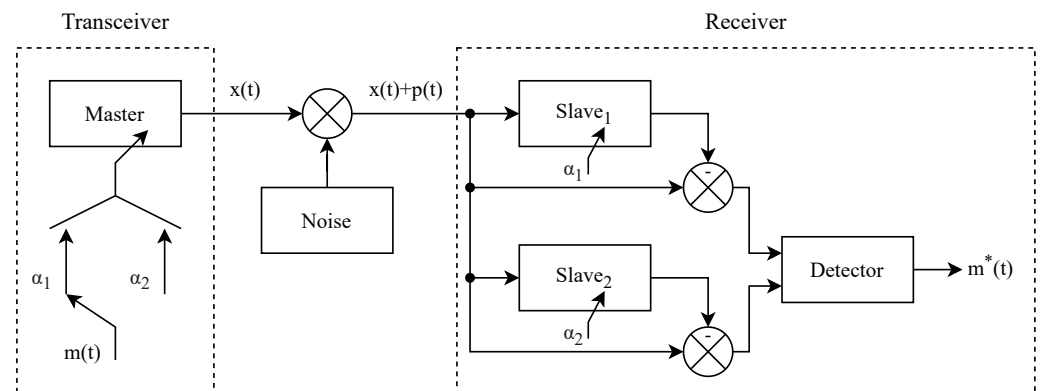


Figure 9. Block diagram of the communication system with RK-alpha.

In this study, we use the well-known Pecora–Carroll method [14] to synchronize chaotic oscillators. We add Pecora–Carroll synchronization to the model and obtain the following finite-difference scheme for the slave (receiver) oscillator:

$$\begin{aligned}
 \dot{x} &= y + xy - yz; \\
 \dot{y} &= x + ayz + k(y_M - y); \\
 \dot{z} &= by^2 + xy;
 \end{aligned}
 \tag{11}$$

where k is the coupling strength coefficient, and y_M is the second variable of the master system. The resulting receiver system, obtained by the RK-alpha method 5, is as follows:

$$\begin{aligned}
 h_\alpha &= \alpha * h; \\
 x_{n+\alpha} &= x_n + h_\alpha(y_n + x_n y_n - y_n z_n); \\
 y_{n+\alpha} &= y_n + h_\alpha(x_n + ay_n z_n + k(y_M - y_n)); \\
 z_{n+\alpha} &= z_n + h_\alpha(by_n^2 + x_n y_n); \\
 x_{n+1} &= x_n + h(\alpha_1 * (y_n + x_n y_n - y_n z_n) + \alpha_2 * (y_{n+\alpha} + x_{n+\alpha} y_{n+\alpha} - y_{n+\alpha} z_{n+\alpha})); \\
 y_{n+1} &= x_n + h(\alpha_1 * (x_n + ay_n z_n) + \alpha_2 * (x_{n+\alpha} + ay_{n+\alpha} z_{n+\alpha}) + k(y_M - y_n)); \\
 z_{n+1} &= x_n + h(\alpha_1 * (by_n^2 + x_n y_n) + \alpha_2 * (by_{n+\alpha}^2 + x_{n+\alpha} y_{n+\alpha})).
 \end{aligned}
 \tag{12}$$

Using the approach reported in [47,49], we have determined that variable Y is the most optimal for synchronization and has a nearly optimal synchronization coefficient of $k = 4$.

The example of a test message (1010110010) transmission by the considered chaotic communication system with RK-alpha modulation is shown in Figure 10.

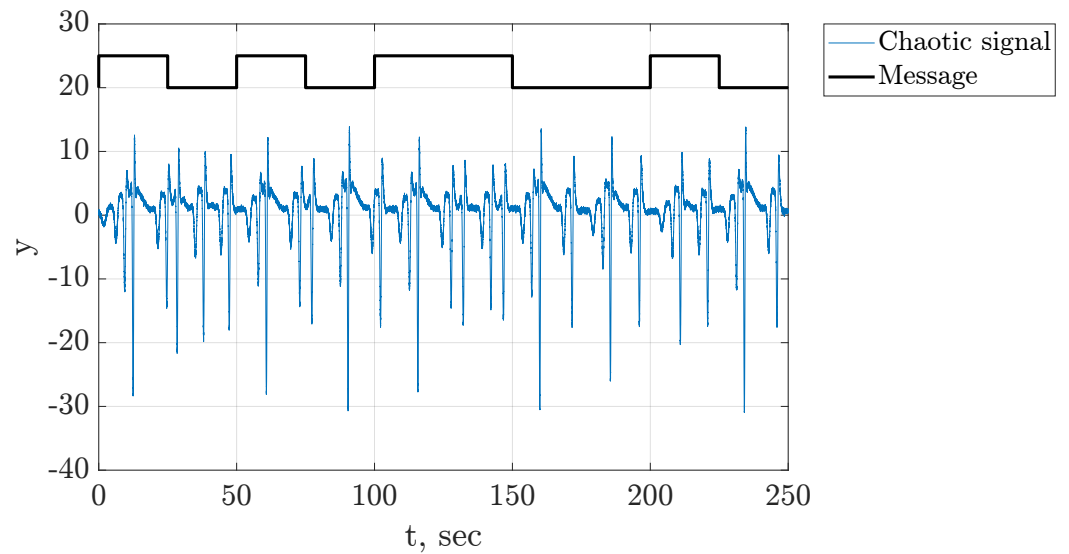


Figure 10. Message transmission.

The dynamics of the synchronization error at the receiver side upon receiving the message (1010110010) with RK-alpha is shown in Figure 11.

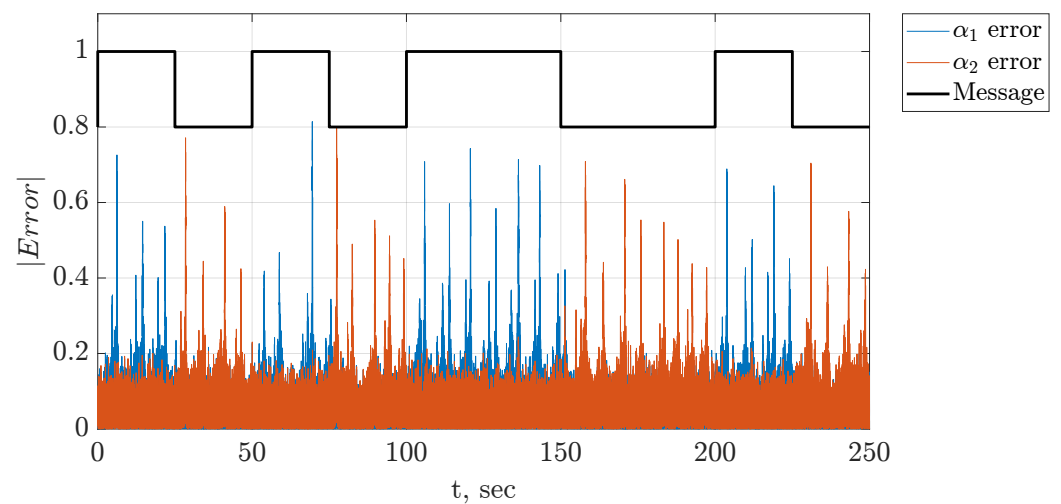


Figure 11. Synchronization error on the receiver side, $\alpha_1 = -54$ and $\alpha_2 = 55$, SNR = 35 dB.

3.1. Experimental Setup

This section provides an overview of the experimental setup designed using the Arduino Due microcontroller and the Integrated Development Environment (IDE) for software development. The Arduino Due microcontroller offers significant advantages for prototyping electronic systems, such as an integrated 12-bit analog-to-digital converter (ADC) and digital-to-analog converter (DAC). The relatively low bit resolution of the DAC/ADC may not be sufficient for the correct working of a chaotic communication system when the spread of modulation parameters is relatively small. However, in our study, the noise from quantization is much lower than the noise in the communication channel, and the set of modulation parameters under investigation are sufficient for 12-bit quantization of DAC/ADC and do not affect the quality of message transmission. The use of high-performance platforms such as Raspberry Pi [29,50] and FPGA [51–53] with higher-bit resolutions of DAC/ADC can increase the quantitative characteristics of the communication system. However, this work is aimed at assessing the qualitative characteristics and presenting a modulation method that has not previously been described in the scientific literature.

The experimental test bench consists of two Arduino Due controllers, an oscilloscope, a keyboard, and two displays. DAC and ADC inputs and outputs are connected to the breadboard. In addition, an adder is placed between the DAC and ADC to introduce additive white noise if needed. This feature is used to investigate the noise immunity of the communication system [54].

We used the integrated DAC and ADC of two Arduino Due microcontrollers to establish analog communication over wired channels. A 4×4 matrix keyboard was used for system parameter configuration. Diodes were installed into the keyboard connector to ensure correct operation when multiple keys in the same column were pressed simultaneously. We also used two 0.96" OLED displays to facilitate parameter setting and monitor message transmission. To introduce white noise into our signal, we placed a signal adder on a breadboard. The adder consists of a Texas Instruments OPA2134 operational amplifier and 51 kOhm resistors. A noise generator (Keysight 33210A) was used to combine the white noise with the signal. An oscilloscope was used to monitor the signal [54].

Below is the code describing the transmitter and receiver chaotic oscillators for the Arduino platform.

The transmitter code is as follows (Listings 1 and 2):

Listing 1. Transmitter code.

```

1 double Ampl = 40;
2 double Mult = 2048 / Ampl;
3 double Delta = 2047;
4
5 void set() {
6   h1 = h * alpha;
7   alpha2 = 1 / (2 * alpha);
8   alpha1 = 1 - alpha2;
9   X1[0] = X[0] + h1 * (X[1] + X[0] * X[1] - X[1] * X[2]);
10  X1[1] = X[1] + h1 * (X[1] + a[0] * X[1] * X[2]);
11  X1[2] = X[2] + h1 * (a[1] * X[1] * X[1] + X[0] * X[1]);
12  X[0] = X[0] + h * (alpha1 * (X[1] + X[0] * X[1] - X[1] * X[2]) +
13    alpha2 * (X1[1] + X1[0] * X1[1] - X1[1] * X1[2]));
14  X[1] = X[1] + h * (alpha1 * (X[1] + a[0] * X[1] * X[2]) +
15    alpha2 * (X1[1] + a[0] * X1[1] * X1[2]));
16  X[2] = X[2] + h * (alpha1 * (a[1] * X[1] * X[1] + X[0] * X[1]) +
17    alpha2 * (a[1] * X1[1] * X1[1] + X1[0] * X1[1]));
18
19  output = X[1] * Mult + Delta;
20  analogWrite(DACO, output);
21 }

```

The receiver code is as follows:

Listing 2. Receiver code.

```

1 double Ampl = 40;
2 double Mult = Ampl / 2048;
3 double Delta = 2047;
4
5 void set() {
6   data = 1.46774194 * (analogRead(A0) - 720);
7   input = (data - Delta) * Mult;
8   Error = input - X[1];
9   synchro = K * Error;
10
11  h1 = h * alpha;
12  alpha2 = 1 / (2 * alpha);
13  alpha1 = 1 - alpha2;
14  X1[0] = X[0] + h1 * (X[1] + X[0] * X[1] - X[1] * X[2]);
15  X1[1] = X[1] + h1 * (X[1] + a[0] * X[1] * X[2] + synchro);
16  X1[2] = X[2] + h1 * (a[1] * X[1] * X[1] + X[0] * X[1]);
17  X[0] = X[0] + h * (alpha1 * (X[1] + X[0] * X[1] - X[1] * X[2]) +
18    alpha2 * (X1[1] + X1[0] * X1[1] - X1[1] * X1[2]));
19  X[1] = X[1] + h * (alpha1 * (X[1] + a[0] * X[1] * X[2]) +
20    alpha2 * (X1[1] + a[0] * X1[1] * X1[2]) + synchro);
21  X[2] = X[2] + h * (alpha1 * (a[1] * X[1] * X[1] + X[0] * X[1]) +
22    alpha2 * (a[1] * X1[1] * X1[1] + X1[0] * X1[1]));
23 }

```

3.2. Bit Error Rate Analysis

The communication system under investigation uses a binary alphabet to transmit messages, where each character corresponds to a particular value of the parameter or value of α . Our experiments included three sets of parameters and values of alpha for the transmission of binary messages. The values of the corresponding sets of parameters are listed in Table 1.

Table 1. Set of modulation parameters for experimental cases.

	αM			PM		
	α_1	α_2	$\Delta\alpha$	a_1	a_2	Δa
Case 1	−24	25	49	0.1	0.0965	0.0035
Case 2	−34	35	69	0.1	0.09525	0.00475
Case 3	−54	55	109	0.1	0.094	0.006

Let us perform a classical BER analysis using direct error counting for the ranges of parameters and α values given in Table 1. It should be noted that we used a relatively small range of parameters for the system, resulting in relatively low noise immunity [54], because in this study, we focused on investigating a CCS with a certain low level of noise immunity with the purpose of disclosure of the most covert modulation technique.

The results are shown in Figure 12, and the BER analysis was performed for 10,000 bits using the chaotic communication test bench described in Section 3.1.

The results of the experiments show that two of three experimental cases (namely, PM case 1 and αM case 2; PM case 2 and αM case 3) possess similar noise immunity. In addition, the selected coefficients for VMM and SCM provide almost identical noise immunity in all cases. Taking into account the similar level of noise immunity of all investigated techniques, one can conclude that the proposed modulation method is potentially superior for secrecy of transmission. Secrecy analysis is performed in the next subsection.

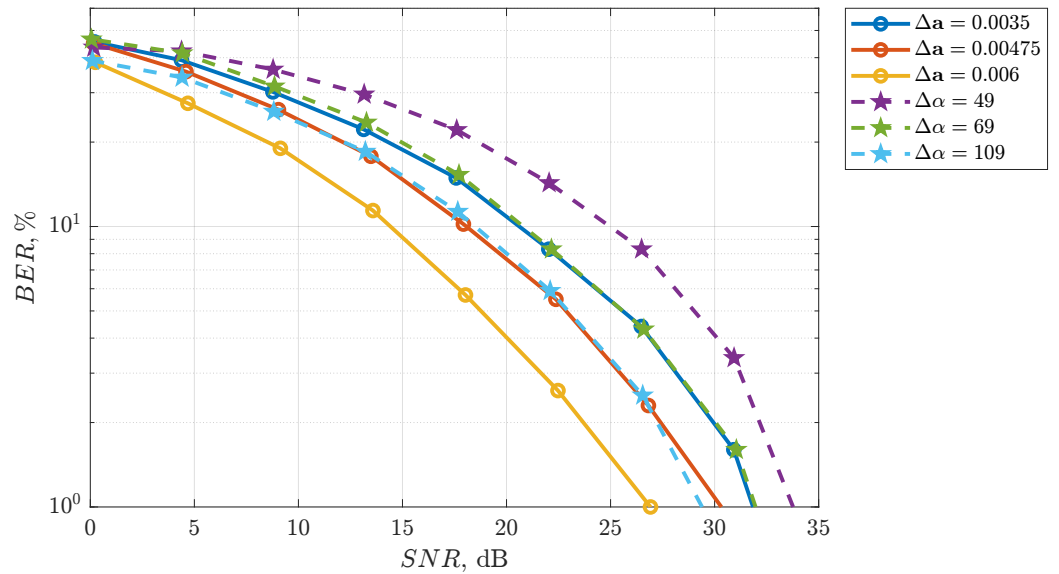


Figure 12. BER vs. SNR estimation.

3.3. Quantified Return Map Analysis (QRMA)

This subsection describes the evaluation of the secrecy of the designed chaotic communication system using specialized analysis methods and software. The underlying algorithm is a further development of the well-known return map analysis method. Let us apply the QRMA method that was described in [43]. To evaluate the secrecy of transmission using this method, one should find the values of the local maxima of the signal amplitude and determine the intervals between them. One point on the desired return map can be obtained by using a pair of values: the value of the maxima and the interval between the two peaks. The first maximum is omitted. Figure 13 displays the signal with the marked maxima.

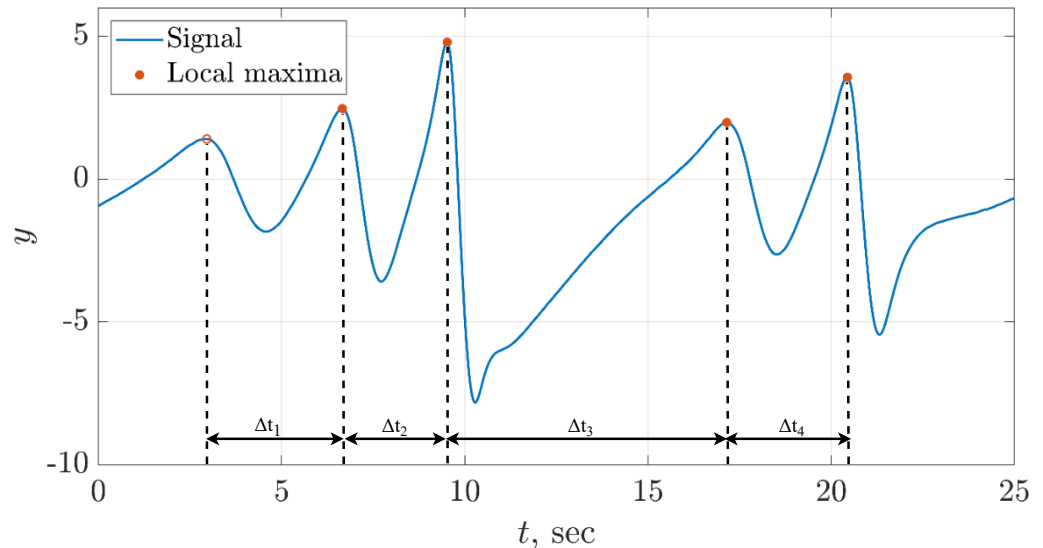


Figure 13. Signal with mapped maximums and inter-peak intervals.

The return maps of the chaotic signal for PM for the third experimental case without noise in the communication channel are in Figure 14. The return maps of the parameters differ from each other, indicating that this set of parameters lacks confidentiality.

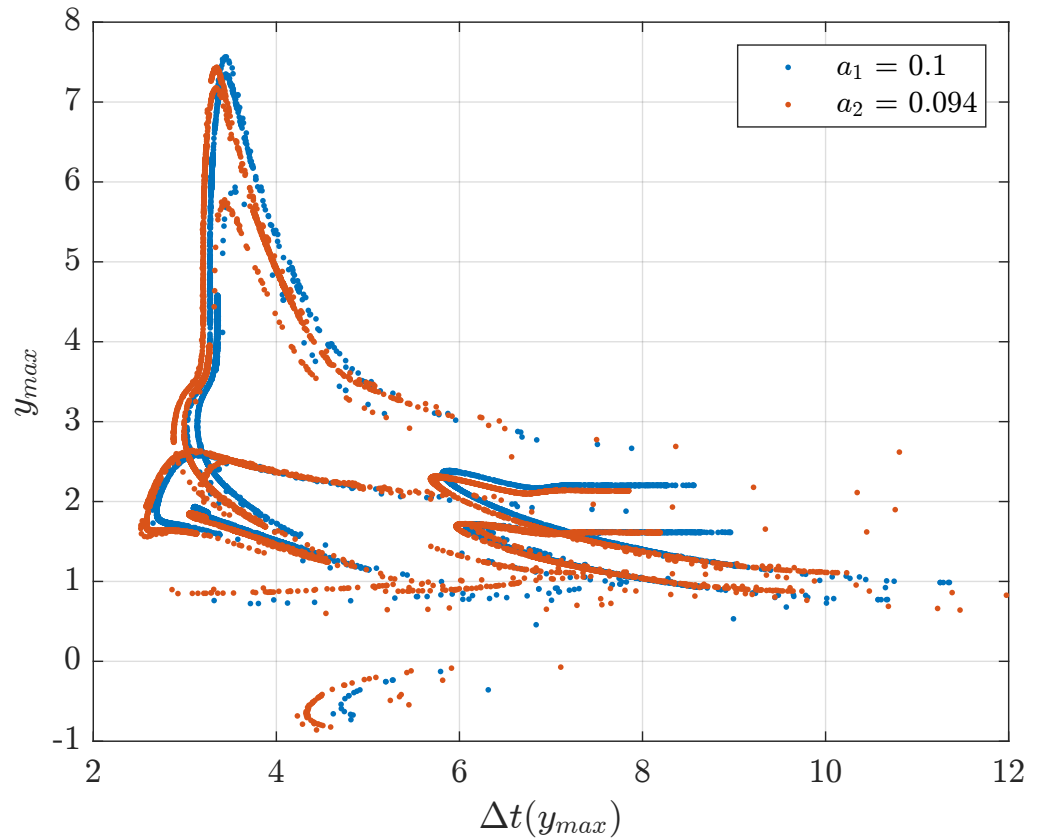


Figure 14. Return map of the chaotic signal for PM.

The following formulae are used to calculate the difference between two return maps:

$$\theta(x) = \begin{cases} x & x \geq \epsilon; \\ 0 & x < \epsilon. \end{cases} \quad \epsilon \in \mathbb{N}_1; \tag{13}$$

$$\Delta_{i,j} = |X_{i,j} - Y_{i,j}| \cdot |\Theta(X_{i,j}) - \Theta(Y_{i,j})|, \quad i, j \in [1, N]; \tag{14}$$

$$D = \sum_{i=1}^N \sum_{j=1}^N \frac{\theta(\Delta_{i,j})}{\theta(X_{i,j}) + \theta(Y_{i,j})}, \tag{15}$$

where Θ is the Heaviside step function, N ($N \times N$) is the 2D histogram resolution, and ϵ is a threshold for cutting off divergent points that affect the calculation of the difference between two return maps [43]. In all our calculations, we define the resolution of the 2D histogram as $N = 80$ and $\epsilon = 3$.

Quantified return map analysis was applied to transmissions conducted with different signal-to-noise ratios and various ranges of α and parameter value variations. We investigate the secrecy of chaotic communications implemented using α M and PM modulation techniques. Figure 15 displays the obtained results.

The experimental results for security evaluation show that the proposed α M technique outperforms the broadly used PM modulation in all considered scenarios.

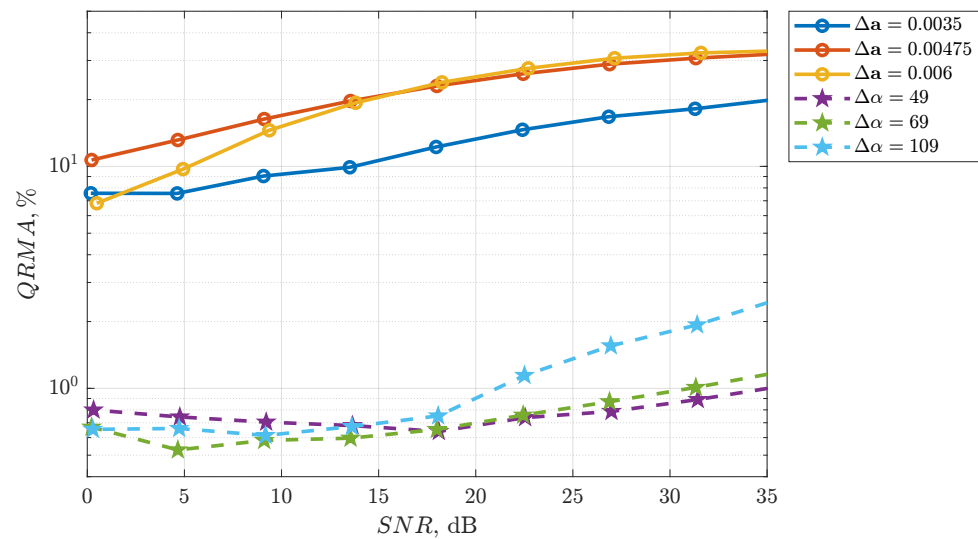


Figure 15. QRMA vs. SNR estimation.

4. Conclusions

In this study, we investigated the dynamics of the Gokyildirim chaotic system discretized by the generalized explicit second-order Runge–Kutta integration method. Using the bifurcation diagrams, Lyapunov spectrum, and basin of attraction analysis, we discovered multistable behavior within a certain range of α values in the discrete Gokyildirim system. Taking this knowledge into account, we developed a novel chaotic signal modulation technique based on changing the value of α in discrete chaotic maps obtained by the generalized explicit second-order Runge–Kutta solver. This technique has potential applications in various fields of chaotic communications and chaos generation as it is suitable for controlling the properties of generated chaotic sequences. We applied quantified return map analysis and bit error rate analysis to the prototyped chaotic communication systems to evaluate the efficiency of the proposed modulation technique. Our analysis showed that the proposed modulation method is suitable for secure data transmission in chaos-based communication systems. An experimental test bench was designed to investigate and compare the suggested modulation method with state-of-the-art chaos modulation techniques. The test bench includes a transmitter, receiver, and noise modules. The experimental results demonstrate that the proposed α -based modulation has high noise resistivity and secrecy, especially when compared to the conventional parameter modulation (PM) approach. A chaotic communication system based on α modulation outperforms its counterpart with parameter modulation by 10–15% in terms of secrecy in all experimental cases and has similar noise immunity. Therefore, it can be concluded that the proposed α -based modulation technique is a simple and versatile method for constructing secure and noise-resistant transceivers for and receivers of chaotic signals for the implementation of chaos-based secure communication systems. The known limitations of the proposed technique can be formulated as follows. The alpha-RK-method-based modulation can be applied only to chaotic oscillators that are described by ODEs. The applicability of this technique to systems described by algebraic differential equations is questionable, and it is certainly not applicable to systems represented by discrete maps. In addition, the technique is fairly useless for noncoherent chaotic communications. The possible directions for future research include designing chaos generators based on fractional-order or stochastic differential equations.

Author Contributions: Conceptualization, D.B.; data curation, V.A.; formal analysis, V.R., V.A. and T.K.; investigation, I.B. and V.R.; methodology, T.K. and D.B.; project administration, T.K.; software, I.B. and V.R.; supervision, D.B.; validation, I.B., V.R., V.A., T.K. and D.B.; visualization, I.B.; writing—original draft, I.B., V.R. and D.B.; writing—review and editing, V.A. and T.K. All authors have read and agreed to the published version of the manuscript.

Funding: This study was supported by the Russian Science Foundation (RSF), project 20-79-10334.

Data Availability Statement: No new data were created or analyzed in this study. Data sharing is not applicable to this article.

Acknowledgments: The authors are grateful to Sergey Kuzmin for his time and fruitful discussions on the topic of this research.

Conflicts of Interest: The authors declare no conflicts of interest.

References

1. Kaddoum, G. Wireless chaos-based communication systems: A comprehensive survey. *IEEE Access* **2016**, *4*, 2621–2648. [[CrossRef](#)]
2. Lorenz, E.N. Deterministic nonperiodic flow. *J. Atmos. Sci.* **1963**, *20*, 130–141. [[CrossRef](#)]
3. Pareek, N.K.; Patidar, V.; Sud, K.K. Image encryption using chaotic logistic map. *Image Vis. Comput.* **2006**, *24*, 926–934. [[CrossRef](#)]
4. Phatak, S.; Rao, S.S. Logistic map: A possible random-number generator. *Phys. Rev. E* **1995**, *51*, 3670. [[CrossRef](#)] [[PubMed](#)]
5. Donati, S.; Hwang, S.K. Chaos and high-level dynamics in coupled lasers and their applications. *Prog. Quantum Electron.* **2012**, *36*, 293–341. [[CrossRef](#)]
6. Terry, J.R.; Thornburg, K.S., Jr.; DeShazer, D.J.; VanWiggeren, G.D.; Zhu, S.; Ashwin, P.; Roy, R. Synchronization of chaos in an array of three lasers. *Phys. Rev. E* **1999**, *59*, 4036. [[CrossRef](#)]
7. Arecchi, F.; Lippi, G.; Puccioni, G.; Tredicce, J. Deterministic chaos in laser with injected signal. *Opt. Commun.* **1984**, *51*, 308–314. [[CrossRef](#)]
8. Chua, L.O. Chua's circuit 10 years later. *Int. J. Circuit Theory Appl.* **1994**, *22*, 279–305. [[CrossRef](#)]
9. Adiyaman, Y.; Emiroglu, S.; Uçar, M.K.; Yildiz, M. Dynamical analysis, electronic circuit design and control application of a different chaotic system. *Chaos Theory Appl.* **2020**, *2*, 10–16.
10. Lin, H.; Wang, C.; Deng, Q.; Xu, C.; Deng, Z.; Zhou, C. Review on chaotic dynamics of memristive neuron and neural network. *Nonlinear Dyn.* **2021**, *106*, 959–973. [[CrossRef](#)]
11. Jovic, B. *Synchronization Techniques for Chaotic Communication Systems*; Springer: Berlin/Heidelberg, Germany, 2011.
12. Baptista, M.S. Chaos for communication. *Nonlinear Dyn.* **2021**, *105*, 1821–1841. [[CrossRef](#)]
13. Wang, L.; Mao, X.; Wang, A.; Wang, Y.; Gao, Z.; Li, S.; Yan, L. Scheme of coherent optical chaos communication. *Opt. Lett.* **2020**, *45*, 4762–4765. [[CrossRef](#)] [[PubMed](#)]
14. Pecora, L.M.; Carroll, T.L. Synchronization in chaotic systems. *Phys. Rev. Lett.* **1990**, *64*, 821. [[CrossRef](#)]
15. Yassen, M. Controlling chaos and synchronization for new chaotic system using linear feedback control. *Chaos Solitons Fractals* **2005**, *26*, 913–920. [[CrossRef](#)]
16. Vargas, J.A.; Grzeidak, E.; Gularte, K.H.; Alfaro, S.C. An adaptive scheme for chaotic synchronization in the presence of uncertain parameter and disturbances. *Neurocomputing* **2016**, *174*, 1038–1048. [[CrossRef](#)]
17. Voznesensky, A.; Butusov, D.; Rybin, V.; Kaplun, D.; Karimov, T.; Nepomuceno, E. Denoising Chaotic Signals Using Ensemble Intrinsic Time-Scale Decomposition. *IEEE Access* **2022**, *10*, 115767–115775. [[CrossRef](#)]
18. Ostrovskii, V.Y.; Rybin, V.G.; Karimov, A.I.; Butusov, D.N. Inducing multistability in discrete chaotic systems using numerical integration with variable symmetry. *Chaos Solitons Fractals* **2022**, *165*, 112794. [[CrossRef](#)]
19. Babajans, R.; Cirjulina, D.; Kolosovs, D.; Litvinenko, A. Quadrature Chaos Phase Shift Keying Communication System Based on Vilnius Chaos Oscillator. In Proceedings of the 2022 Workshop on Microwave Theory and Techniques in Wireless Communications (MTTW), Riga, Latvia, 5–7 October 2022; pp. 5–8.
20. Ouannas, A.; Karouma, A.; Grassi, G.; Pham, V.T. A novel secure communications scheme based on chaotic modulation, recursive encryption and chaotic masking. *Alex. Eng. J.* **2021**, *60*, 1873–1884. [[CrossRef](#)]
21. Leung, H.; Lam, J. Design of demodulator for the chaotic modulation communication system. *IEEE Trans. Circuits Syst. Fundam. Theory Appl.* **1997**, *44*, 262–267. [[CrossRef](#)]
22. Karimov, T.; Rybin, V.; Kolev, G.; Rodionova, E.; Butusov, D. Chaotic Communication System with Symmetry-Based Modulation. *Appl. Sci.* **2021**, *11*, 3698. [[CrossRef](#)]
23. Fang, Y.; Han, G.; Chen, P.; Lau, F.C.; Chen, G.; Wang, L. A survey on DCSK-based communication systems and their application to UWB scenarios. *IEEE Commun. Surv. Tutorials* **2016**, *18*, 1804–1837. [[CrossRef](#)]
24. Galias, Z.; Maggio, G.M. Quadrature chaos-shift keying: Theory and performance analysis. *IEEE Trans. Circuits Syst. Fundam. Theory Appl.* **2001**, *48*, 1510–1519. [[CrossRef](#)]
25. Estudillo-Valdez, M.A.; Adeyemi, V.A.; Nuñez-Perez, J.C. FPGA realization of an image encryption system using the DCSK-CDMA technique. *Integration* **2024**, *96*, 102157. [[CrossRef](#)]
26. Pisarchik, A.N.; Jaimes-Reátegui, R.; Rodríguez-Flores, C.; García-López, J.; Huerta-Cuéllar, G.; Martín-Pasquín, F.J. Secure chaotic communication based on extreme multistability. *J. Frankl. Inst.* **2021**, *358*, 2561–2575. [[CrossRef](#)]
27. Chan, J.C.L.; Lee, T.H.; Tan, C.P. Secure communication through a chaotic system and a sliding-mode observer. *IEEE Trans. Syst. Man Cybern. Syst.* **2020**, *52*, 1869–1881. [[CrossRef](#)]
28. Bian, Y.; Yu, W. A secure communication method based on 6-D hyperchaos and circuit implementation. *Telecommun. Syst.* **2021**, *77*, 731–751. [[CrossRef](#)]

29. Martínez-Fuentes, O.; Díaz-Muñoz, J.D.; Muñoz-Vázquez, A.J.; Tlelo-Cuautle, E.; Fernández-Anaya, G.; Cruz-Vega, I. Family of controllers for predefined-time synchronization of Lorenz-type systems and the Raspberry Pi-based implementation. *Chaos Solitons Fractals* **2024**, *179*, 114462. [[CrossRef](#)]
30. Cirjulina, D.; Babajans, R.; Capligins, F.; Kolosovs, D.; Litvinenko, A. Experimental Study on Colpitts Chaotic Oscillator-Based Communication System Application for the Internet of Things. *Appl. Sci.* **2024**, *14*, 1180. [[CrossRef](#)]
31. Ilyas, B.; Raouf, S.M.; Abdelkader, S.; Camel, T.; Said, S.; Lei, H. An efficient and reliable chaos-based iot security core for udp/ip wireless communication. *IEEE Access* **2022**, *10*, 49625–49656. [[CrossRef](#)]
32. Sadoudi, S.; Azzaz, M.S.; Djeddou, M.; Benssalah, M. An FPGA real-time implementation of the Chen's chaotic system for securing chaotic communications. *Int. J. Nonlinear Sci.* **2009**, *7*, 467–474.
33. ŞAHİN, M.; Guler, H.; HAMAMCI, S. Design and realization of a hyperchaotic memristive system for communication system on FPGA. *Trait. Signal* **2020**, *37*, 939–953. [[CrossRef](#)]
34. Elsafty, A.H.; Tolba, M.F.; Said, L.A.; Madian, A.H.; Radwan, A.G. Enhanced hardware implementation of a mixed-order nonlinear chaotic system and speech encryption application. *Int. J. Electron. Commun.* **2020**, *125*, 153347. [[CrossRef](#)]
35. Pano-Azucena, A.; Tlelo-Cuautle, E.; Rodriguez-Gomez, G.; De La Fraga, L. FPGA-based implementation of chaotic oscillators by applying the numerical method based on trigonometric polynomials. *Aip Adv.* **2018**, *8*, 075217. [[CrossRef](#)]
36. TL, C.; LM, P. Synchronizing chaotic circuits. *IEEE Trans. Circuits Syst.* **1991**, *38*, 453–456.
37. Babajans, R.; Cirjulina, D.; Kolosovs, D.; Litvinenko, A. Experimental Study on Analog and Discrete Chaos Oscillators Synchronization. In Proceedings of the 2023 Workshop on Microwave Theory and Technology in Wireless Communications (MTTW), Riga, Latvia, 4–6 October 2023; pp. 24–28.
38. Babajans, R.; Cirjulina, D.; Capligins, F.; Kolosovs, D.; Litvinenko, A. Synchronization of Analog-Discrete Chaotic Systems for Wireless Sensor Network Design. *Appl. Sci.* **2024**, *14*, 915. [[CrossRef](#)]
39. Karimov, T.; Butusov, D.; Andreev, V.; Karimov, A.; Tutueva, A. Accurate synchronization of digital and analog chaotic systems by parameters re-identification. *Electronics* **2018**, *7*, 123. [[CrossRef](#)]
40. Shao, W.; Fu, Y.; Cheng, M.; Deng, L.; Liu, D. Chaos Synchronization Based on Hybrid Entropy Sources and Applications to Secure Communication. *IEEE Photonics Technol. Lett.* **2021**, *33*, 1038–1041. [[CrossRef](#)]
41. Tutueva, A.V.; Moysis, L.; Rybin, V.G.; Kopets, E.E.; Volos, C.; Butusov, D.N. Fast synchronization of symmetric Hénon maps using adaptive symmetry control. *Chaos Solitons Fractals* **2022**, *155*, 111732. [[CrossRef](#)]
42. Tutueva, A.; Moysis, L.; Rybin, V.; Zubarev, A.; Volos, C.; Butusov, D. Adaptive symmetry control in secure communication systems. *Chaos Solitons Fractals* **2022**, *159*, 112181. [[CrossRef](#)]
43. Rybin, V.; Butusov, D.; Rodionova, E.; Karimov, T.; Ostrovskii, V.; Tutueva, A. Discovering chaos-based communications by recurrence quantification and quantified return map analyses. *Int. J. Bifurc. Chaos* **2022**, *32*, 2250136. [[CrossRef](#)]
44. Butcher, J.C.; Wanner, G. Runge-Kutta methods: Some historical notes. *Appl. Numer. Math.* **1996**, *22*, 113–151. [[CrossRef](#)]
45. Süli, E.; Mayers, D.F. *An Introduction to Numerical Analysis*; Cambridge University Press: Cambridge, UK, 2003.
46. Ralston, A. Runge-Kutta methods with minimum error bounds. *Math. Comput.* **1962**, *16*, 431–437. [[CrossRef](#)]
47. Rybin, V.; Butusov, D.; Babkin, I.; Pesterev, D.; Arlyapov, V. Some Properties of a Discrete Lorenz System Obtained by Variable Midpoint Method and Its Application to Chaotic Signal Modulation. *Int. J. Bifurc. Chaos* **2024**, *34*, 2450009. [[CrossRef](#)]
48. Gokyildirim, A.; Kocamaz, U.E.; Uyaroglu, Y.; Calgan, H. A novel five-term 3D chaotic system with cubic nonlinearity and its microcontroller-based secure communication implementation. *Int. J. Electron. Commun.* **2023**, *160*, 154497. [[CrossRef](#)]
49. Rybin, V.; Babkin, I.; KVÍTKO, D.; Karimov, T.; Nardo, L.; Nepomuceno, E.; Butusov, D. Estimating Optimal Synchronization Parameters for Coherent Chaotic Communication Systems in Noisy Conditions. *Chaos Theory Appl.* **2023**, *5*, 141–152. [[CrossRef](#)]
50. Guillén-Fernández, O.; Tlelo-Cuautle, E.; de la Fraga, L.G.; Sandoval-Ibarra, Y.; Nuñez-Perez, J.C. An image encryption scheme synchronizing optimized chaotic systems implemented on raspberry pis. *Mathematics* **2022**, *10*, 1907. [[CrossRef](#)]
51. Sambas, A.; Vaidyanathan, S.; Zhang, X.; Koyuncu, I.; Bonny, T.; Tuna, M.; Alçin, M.; Zhang, S.; Sulaiman, I.M.; Awwal, A.M.; et al. A novel 3D chaotic system with line equilibrium: Multistability, integral sliding mode control, electronic circuit, FPGA implementation and its image encryption. *IEEE Access* **2022**, *10*, 68057–68074. [[CrossRef](#)]
52. Tlelo-Cuautle, E.; Carbajal-Gomez, V.; Obeso-Rodelo, P.; Rangel-Magdaleno, J.; Nunez-Perez, J.C. FPGA realization of a chaotic communication system applied to image processing. *Nonlinear Dyn.* **2015**, *82*, 1879–1892. [[CrossRef](#)]
53. Sambas, A.; Miroslav, M.; Vaidyanathan, S.; Ovilla-Martínez, B.; Tlelo-Cuautle, E.; Abd El-Latif, A.A.; Abd-El-Atty, B.; Benkouider, K.; Bonny, T. A New Hyperjerk System with a Half Line Equilibrium: Multistability, Period Doubling Reversals, Antimonotonicity, Electronic Circuit, FPGA Design and an Application to Image Encryption. *IEEE Access* **2024**, *12*, 9177–9194. [[CrossRef](#)]
54. Rybin, V.; Karimov, T.; Bayazitov, O.; Kvitko, D.; Babkin, I.; Shirnin, K.; Kolev, G.; Butusov, D. Prototyping the Symmetry-Based Chaotic Communication System Using Microcontroller Unit. *Appl. Sci.* **2023**, *13*, 936. [[CrossRef](#)]

Disclaimer/Publisher's Note: The statements, opinions and data contained in all publications are solely those of the individual author(s) and contributor(s) and not of MDPI and/or the editor(s). MDPI and/or the editor(s) disclaim responsibility for any injury to people or property resulting from any ideas, methods, instructions or products referred to in the content.